Experiment and Research on Self-sustaining Performance of a 30-kW Micro Gas Turbine Generator System during Startup

Jin Guan [a], Xiaojing Lv [b,*], Catalina Spataru[3], Yiwu Weng*[,*]

[1] Key Laboratory for Power Machinery and Engineering of Ministry of Education, School of Mechanical Engineering, Shanghai Jiao Tong University, Shanghai, 200240, China

[2] China-UK Low Carbon College, Shanghai Jiao Tong University, Shanghai, 201306, China

[3] Energy Institute, University College London, 14 Upper Woburn Place, London, WC1H 0NN, UK

ABSTRACT

The safe startup of micro gas turbine (MGT) generator system is the premise of normal operation. The whole start-up process contains motor startup, ignition, speed acceleration, motor switching to generator and power acceleration. Motor switching to generator happens at the self-sustaining state. MGT crossing self-sustaining boundary is a continuous process and significant to safe start-up process. However, the challenge is that characteristic of MGT generator system at self-sustaining state is hardly to investigate due to the lack of performance maps and complete experiments. Therefore, this work analyzed start-up schedule and presented a theoretical and experimental study on the self-sustaining performance of MGT generator system, based on the self-designed 40 kW MGT generator system built in Jiangjin Turbocharger Plant, China. Designed specifications of the full-scaled MGT include rotational speed of 34,000 rpm, compressor ratio of 2.45 and turbine inlet temperature of 810 ℃. The self-sustaining speed boundary line and operation fuel area are determined from the aspects of turbine safety temperature and motor load capacity. Then, to acquire maximum adjustable

* Corresponding authors.

E-mail addresses: lvxiaojing@sjtu.edu.cn (X. Lv), ywweng@sjtu.edu.cn (Y. Weng).

operation margin during the startup process of the MGT, a novel principle for determining the self-sustaining point (SSP) is proposed. Results show that the self-sustaining state can be achieved only when speed is over 27,050 rpm, and a higher speed can lead to lower turbine inlet temperature (TIT) at self-sustaining state. Meanwhile, the SSP is determined at the speed of 31,850 rpm in the start-up process based on the proposed principle. Finally, the self-sustaining state and operation fuel area of MGT are compared with the experimental data at different environmental temperature and rotational speed, with two relative errors both almost within 4%, which is instructive to the actual startup process.

Key words：Micro gas turbine; Start-up schedule; Self-sustaining boundary; Fuel operation area; Experimental validation

Nomenclatures

MGT	micro gas turbine	kg	average specific heat ratio
T_3, TIT	turbine inlet temperature (℃)	m_1	air mass flow rate (kg/s)
T_1	compressor inlet temperature (℃)	m_2	fuel mass flow rate (kg/s)
T_2	compressor outlet temperature (℃)	m	gas mass flow rate (kg/s)
T_4	turbine outlet temperature (℃)	W_t	turbine outlet power (kW)
W_C	compressor consumption power (kW)	n	Speed (rpm)
c_{p2}	specific heat of gas in the turbine (kJ/kg·k)	V_2	gas volume flow (m^3/s)
P	work consumption of Sliding bearing (kW)	c_{p1}	specific heat of air (kJ/kg·k)
c_{p3}	specific heat of gas in the combustor (kJ/kg·k)	R	bearing radius (m)
U	bearing circumferential velocity (m/s)	c	bearing clearance (m)
R_f	relative adjustment of fuel benchmark	L	bearing width (m)
η	lubricating oil viscosity (Pa/s)	e	eccentricity ratio
π_c	compressor ratio	M	motor power (kW)
η_r	combustion efficiency	η_c	compressor efficiency
η_{cd}	purity of fuel	π_t	turbine expansion ratio
s	total pressure recovery coefficient in combustor	η_t	turbine efficiency

1. Introduction

The global concerns on greenhouse emissions and energy utilization speed up the revolution of energy consumption structure[1, 2]. World Energy Scenarios in 2019 presents the global primary energy consumption from 1978 to 2018. The rise in the total global primary energy consumption within the past 40 years was mainly covered by fossil fuels, above of which the share of gas fuels is increased largely[3-5]. As the main equipment to use gas, gas turbine itself has advantages in compact size, low maintenance requirements, low carbon emissions and fuel flexibility [6-10]. Besides, the application of micro gas turbine (MGT) is more flexible and extensive. MGT is compatible with other energy utilization equipment or recycling system, such as solid oxygen fuel cell, solar energy, organic Rankine cycle or energy storage system[11-15], and the whole system efficiency can be greatly improved. MGT also can be considered as a range extender for electric vehicles[16]. Therefore, MGT has a promising prospect in the energy utilization system [17, 18].

MGT is used as a programmable energy vector for compensating the deficits of renewable energies (such as solar and wind) in a multi-energy grid. MGT needs to dozens of starts and stops on sunny and cloudy days. It is a necessary requirement that MGT has a good performance on the startup[19]. However, although there are many researches on the operation performance of gas turbine[20, 21], researches on startup of gas turbine are not so much. Methods and modeling of startup have been discussed. Forsthoffer [22] summarized the gas turbine startup and shutdown sequencing system in considering of safety, which needed to prevent engine fires or explosions and minimize thermal effects. Besides, it is also necessary to eliminate damage caused by vibration or by air compressor stall surge. David Pritchard[23] established startup and shutdown procedures of MGT and test it over 100 successful starts. The startup time of biomass and gas was recorded. The starting procedure of gas required motoring for less than 2min at most, and the startup time of biomass was for up to 30min. K.A.Al-attab [24] compared two different turbine startup methods in the external fired micro gas turbine (EFMGT). One was to use two air blowers of 5.5 kW and 7.5 kW to increase

the air pressure at the turbine inlet. Another was to use a centrifugal air compressor, which decreased the air heating rate and delayed the startup process but providing much higher air pressure. The result was that centrifugal air compressor was more beneficial for startup of EFMGT. Hamid Asgari[25] developed and validated nonlinear autoregressive exogenous (NARX) models of a heavy-duty single-shaft gas turbine (GT) during the start-up procedure. The models were constructed by using three measured time-series data sets from General Electric PG 9351FA. The resulting NARX models were tested against three other available experimental data sets for verification of the models. The deviation between measured and simulated results is within 7.5% in most cases. J.H.Kim[26] constructed a simulation model of the start-up procedure of heavy duty gas turbines based on the unsteady one-dimensional conservation equations. The dynamic behavior of a 150MW class gas turbine (GE 7F) was simulated for a full start-up procedure from zero to full speed. Poorya Keshavarz Mohammadian [27] developed a transient model to simulate the start-up procedure of an industrial twin-shaft gas turbine. The components' characteristics were generated by CFD simulation tools based on real geometry. The start-up operation was simulated from zero speed to the base load condition and validated with field data. Ping Lin[28] built the modeling of a 135kW micro gas turbine in MATLAB/Simulink environment. The component characteristic map model was established by combining inter-component volume method with experiment data. Start-up process was classified into three stages. Then, polynomial fitting method with identification method were used in the start-up model. The steady-state errors between the experiment data and the simulation data were less than 4%. A.Mehrpanahi [29] discussed the modeling of the start-up and loading modes, which contains the neural network (NN) method and the derived functions of linear regression (LR), Hammerstein-Wiener (HW) fitted structures, and nonlinear auto-regressive exogenous (NARX), shaft dynamic (SD)-based function and the time-delayed transfer functions. It was concluded that shaft speed was the most important factor in determining the noted parameters, and the relative superiority of neural network method to generate a turbine output speed was demonstrated during the startup mode. From the literature above, experimental study on the startup of micro gas turbine is still very

lacked.

During the startup process of MGT generator system, one of the most important stage is the self-sustaining state. The self-sustaining state is the equilibrium point, where motivating torque of turbine and resistance torque of compressor and sliding bearing are equally balanced, and the motor and generator both provide zero output power. It is clear that self-sustaining state marks the boundary of generator and motor and is of significance in the startup process. However, there are few researches on the self-sustaining condition of the micro gas turbine system. Pritchard D [30]took five biomass generator performance tests of MGT. Results showed that when system had leaks in some of the connections, it could not maintain constant rotational speed without electrical assistance. Meanwhile, the authors pointed out that self-sustaining state was closely related with rotational speed. K.A.Al-attab [24] calculated the turbine and compressor plots to check whether the turbine power was more than half the compressor theoretical power or not at half the operation speed when it reached the self-running mode. JeongMin Seo [31] built the 500 W ultra-micro gas turbine (UMGT) generator composed of a centrifugal compressor, a radial turbine, an annular combustor and a shaft to measure the performance of electric-power generation. Tests were conducted to examine the feasibility of start-up and self-sustaining capabilities. Results showed that the self-sustaining condition could be achieved around 120,000rpm and 150,000rpm. Noor Badshah [32] built a externally fired gas turbine and find that the turbine inlet temperature below 700℃ could not meet self-sustaining mode. Then heat exchanger was redesigned, where eight annular tube sizes from inner diameter 6 mm to 20 mm were compared. When tube inner diameter and mild-steel tube inner diameter were 15 mm and 25 mm respectively, turbine inlet temperature could be elevated up to nearly 900℃ and self-sustaining mode could be reached.

As can be seen from the literatures above, all aforementioned studies on the self-sustaining state were carried out at some separated rotating speeds. However, the self-sustaining state with regards to continuous speed changing in the startup process is not analyzed. It is obvious that speed is always continuously changing in the start-up process of MGT generator system in the reality, as shown in **Fig. 1**. Operation line must

go through self-sustaining point (SSP), and then go into generation area till designed point. As a result, the research on some separated self-sustaining state is not so convincible in the startup process of MGT. What's more, it is necessary to predict the operation fuel area in the startup process. Although some researches on startup have been conducted by experiment or theory, the fuel operation area has not been discussed yet. Fuel flowing rate is the most important adjustable variable, which influences TIT and output power of MGT directly. On the one hand, if fuel flowing rate is provided too much, TIT will exceed allowable temperature of material. On the contrary, motor cannot drive the MGT when fuel is too little. On the other hand, after self-sustaining state, enough adjustable range of fuel must be given to match the load, otherwise rotational speed will be changed, which may exceed the speed limit.

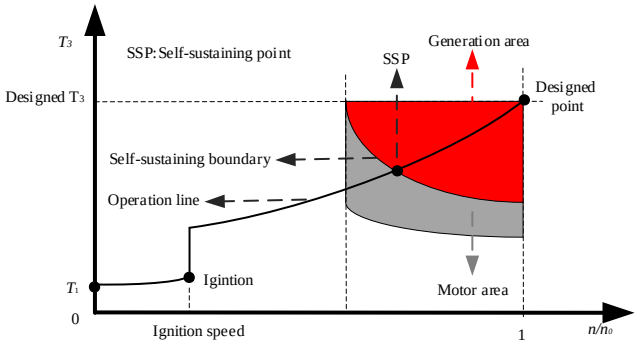

Fig. 1. Operation line through self-sustaining boundary.

Furthermore, how to determine the SSP is also not discussed in current researches on MGT startup. Self-sustaining state is closely related to control strategy of MGT in the start-up process. Before the SSP, speed control mode works. After the SSP, power control mode works. Based on this, there are two modes of start-up process. One is to reach the generation state at the off-design speed, and then continue to promote the speed and generation power to design speed. The other is to reach the design speed first, and then get into the generation state until MGT arrives at design point. Above all, the control mode of MGT system can't be repeatedly switched, otherwise stability of MGT system will be affected. Therefore, it is necessary to determine SSP in the start-up process of MGT system.

To address the questions above, this paper has investigated the startup schedule and

self-sustaining state of MGT generator system in continuous speed based on the self-designed 40kW MGT generator system in Jiangjin Turbocharger Plant, China. The start-up process of MGT generator system from static to generation state was captured and studied, which contains motor startup, ignition, speed acceleration, motor switching to generator and power acceleration. Firstly, the startup schedule is analyzed based on the components' function and operation law of MGT. Secondly, self-sustaining boundary and operation fuel area in the stable state are determined based on the designed parameters of MGT generator system. Characteristics of self-sustaining natural gas, TIT and MGT power related to speed are all analyzed. Then, considering the influence of self-sustaining state on the start-up process, take maximum fuel mass as relative adjustment of fuel benchmark in the motor state. The self-sustaining speed is obtained based on maximum adjustable fuel operation principle. Finally, self-sustaining experiments are carried out at different temperature and speed. Accuracy of model of self-sustaining performance is testified by the experimental data. Meanwhile, operation fuel area is verified by comparing the mass flow of theoretical and experimental natural gas during the startup process.

At present, experimental research on self-sustaining boundary and fuel area of MGT generator system during the startup process has not been fully studied before. The methodology in this work could provide experimental guidance to startup process of MGT generator system, which would also facilitate its implementation in multi-energy system or distributed power generation. As a result, the main contribution of the present work could be summarized as follows:

- Self-sustaining boundary and fuel area are determined based on the characteristic map and operation constraints of MGT generator system during the startup process.
- A novel principle for determining the self-sustaining point is proposed based on the principle of maximum adjustable fuel operation area.
- Experimental tests at different environmental temperature and speed are conducted and the error analysis between experimental data and calculations are made.

2. Specifications of micro gas turbine generator system

Shanghai Jiao Tong University collaborates with Chongqing jiang zeng corporation to design and build 40 kW MGT power generator system. The system structure is shown in the **Fig. 2**. Power is generated and converted into electricity, which can be uploaded to the power grid or supplied to load. **Table 1** shows the designed parameters if MGT generator system. MGT generator system is composed of a radial turbine, a centrifugal compressor, a combustion chamber, a permanent magnet motor, a control system, and a sliding bearing with lubrication system. Turbine shares a bearing with compressor, which is an intermediate support structure. Air is pressurized in the compressor. Fuel is burned with air in the combustor to evaluate gas temperature and then enters the turbine to expand and produce power. The power is used to drive compressor to induce atmosphere and sends it into combustion chamber. Permanent magnet motor works as motor and generator. When turbine provides power less than compressor and sliding bearing consumption, motor will work to compensate power. On the contrary, if turbine provides more power than compressor and sliding bearing consumption, generator will work to produce net generation. Generator is linked with coupling extended from compressor end to make generation. The value of load is set in the computer, which controls the generator output power. The controller system makes sure power of motor actively match the MGT.

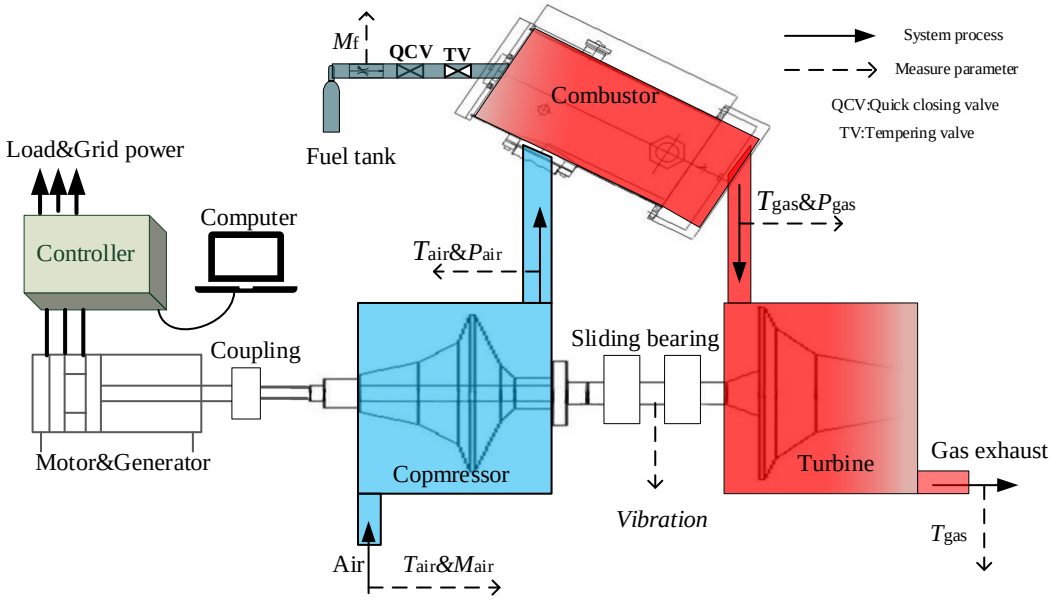

Fig. 2. The structure of Micro gas turbine power generator system.

According to the structure of MGT power generator system, main thermal parameters have been measured. The dotted line in **Fig. 2** represents measured parameters. Temperature of inlet and outlet of compressor and turbine is measured by PT100. The air flow rate into the compressor is measured by orifice flowmeter. Frost technology thermal flowmeter is used to regulate and measure the natural gas flow rate. The outlet air pressure of compressor is measured by mercury gauge. However, due to the high temperature, the gas pressure of outlet of combustor is measured by PGT701.

Table 1

Designed parameters of MGT generator system.

Parameter	Value
Rotational speed of shaft	34,000 rpm
Mass flow rate of inlet air	0.97 kg/s
Temperature of inlet air	25 ℃
Pressure ratio of compressor	2.45
Pressure ratio of turbine	2.33
Compressor isentropic efficiency	0.64
Combustor efficiency	0.98
Total pressure recovery coefficient of combustor	0.95
Turbine inlet temperature	810 ℃
Turbine isentropic efficiency	0.68
Motor power	30 kW

What's more, there are several sensors and valves to monitor and assure MGT safety. Quick closing valve and tempering valve are both placed before the inlet of the combustion chamber, as shown in **Fig. 2**. When the speed exceeds the maximum speed or the turbine inlet temperature is over the maximum allowable temperature, the quick closing valve works to shut down the fuel supply immediately. Tempering valve is to avoid the flame from the combustion chamber into the gas tank. There is bentley vibration sensor to monitor the vibration because the high vibration may be caused at critical speed, which damages the MGT. The temperature of lubrication oil is also measured to monitor the temperature of slider bearing. The real MGT power generator system is shown in **Fig. 3**.

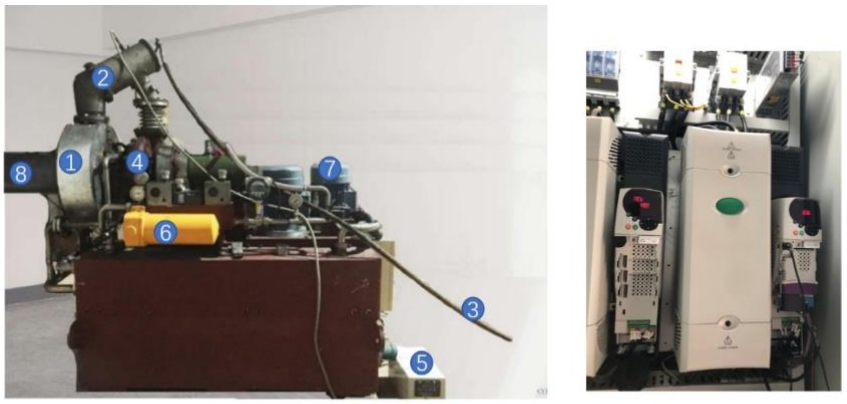

Micro gas turbine PLC controller

1.turbine 2.combustor 3. gas intake line 4.compressor 5. igniter 6. filter 7. oil pump 8. exhaust

Fig. 3. Micro gas turbine generator system.

3. Methodology

3.1 Start-up Schedule of MGT Generator System

As mentioned above, the whole start-up process contains motor startup, ignition, speed acceleration, motor switching to generator and power acceleration. **Fig. 4** depicts the relationship between T_3 and turbine reduced speed n/ n_0 during the startup**.** Combining components' function with operation law of MGT, the startup schedule of MGT can be divided into three stages. The first stage is motor startup from zero to ignition speed. Motor supplies power to counteract the consumption power of compressor and sliding bearing to drive the MGT to operate. At the ignition speed, fuel

is ignited and burned with air in the combustor. This causes the turbine inlet temperature to rise sharply and turbine begins to produce power. The second stage is speed acceleration from ignition speed to self-sustaining speed, where turbine speed is accelerated under the joint action of turbine and motor. The third stage is that speed and power acceleration from self-sustaining speed to designed point, where MGT has three paths. The three paths divided is associated with the working state of permanent magnet motor. The first path is that MGT operates in the generation state, where generator works. Turbine speed and net power are both promoted in this path. The second path is that turbine speed is accelerated to nominal speed without the help of motor, where MGT is always keep self-sustaining, and then net power is enhanced to designed power at the nominal speed. The third path is that MGT never reaches the self-sustaining state motor keeps work before the nominal speed. Self-sustaining state is got at the nominal speed, and then net power is enhanced to designed power.

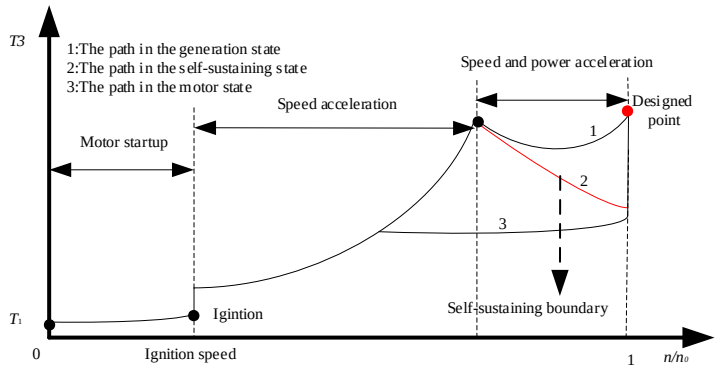

Fig. 4. Turbine inlet temperature during the startup process.

3.2 Micro gas turbine mathematical model

3.2.1 Compressor

Pressure ratio π_c and isentropic efficiency η_c are the key performance parameters, which are always provided from compressor performance map. **Fig. 5** shows the performance of compressor. Compressor itself has many operation paths from zero to full speed if it has inlet guide vane (IGV). However, there is no IGV in the MGT. Therefore, it has only one operation schedule. Pressure ratios is function of speed.

According to the atmosphere temperature and pressure, pressure ratio and corrected rotational speed $n/\sqrt{T_1}$ can be calculated. Then, isentropic efficiency and corrected mass flow $m_1\sqrt{T_1}/P_1$ can be obtained from the compressor performance map. Work consumption of compressor can be calculated by Eq (1). The work consumption is calculated by the difference of inlet and outlet temperature of compressor in the experiment, as shown in Eq (2).

$$W_C = m_1 * c_{p1} * T_1 * (\pi_c^{\frac{kg-1}{kg}} - 1) / \eta_c \tag{1}$$

$$W_C = m_1 * c_{p1} * (T_2 - T_1) / \eta_c \tag{2}$$

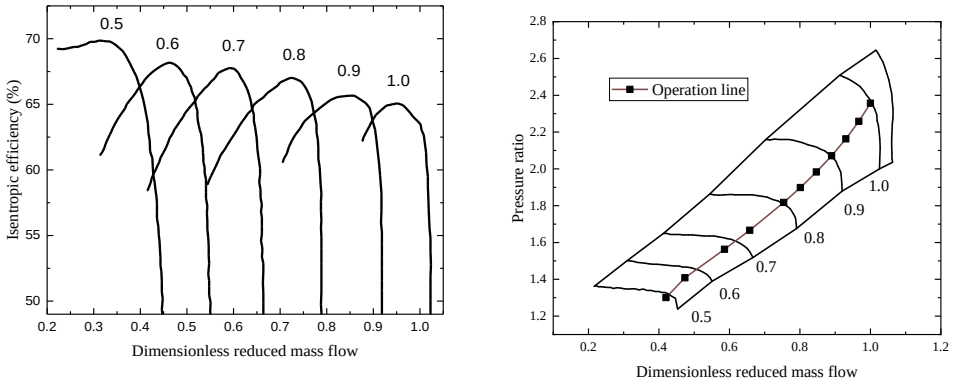

Fig. 5. Performance of compressor.

3.2.2 Combustor

Chemical energy is converted into heat energy to increase TIT in the combustor. The mass balance equation is that gas comprises of fuel and air, as seen from Eq (3).

$$m_1 + m_f = m_3 \tag{3}$$

The energy balance equation is governing the performance of the combustor as follows Eq (4):

$$m_1 \cdot c_{p1} \cdot T_2 + m_f \cdot LHV \cdot \eta_f = m_3 \cdot c_{p3} \cdot T_3 \tag{4}$$

where *LHV* denotes the low heat value of natural gas used.

3.2.3 Turbine

Similar to the compressor, turbine performance is represented by turbine characteristic maps that present the interrelationships between turbine pressure ratio π_t, corrected mass flow $m_3\sqrt{T_3}/P_3$, corrected rotational speed $n/\sqrt{T_3}$ and efficiency η_t. **Fig. 6** gives the map of turbine performance based on the real turbine. The turbine output work is calculated in the theory by Eq (5) and that is calculated in the experiment by Eq (6).

$$W_t = (m_1 + m_2) * c_{p2} * T_3 * (1 - \pi_t^{-\frac{kg-1}{kg}}) * \eta_t \tag{5}$$

$$W_t = (m_1 + m_2) * c_{p2} * (T_3 - T_4) * \eta_t \tag{6}$$

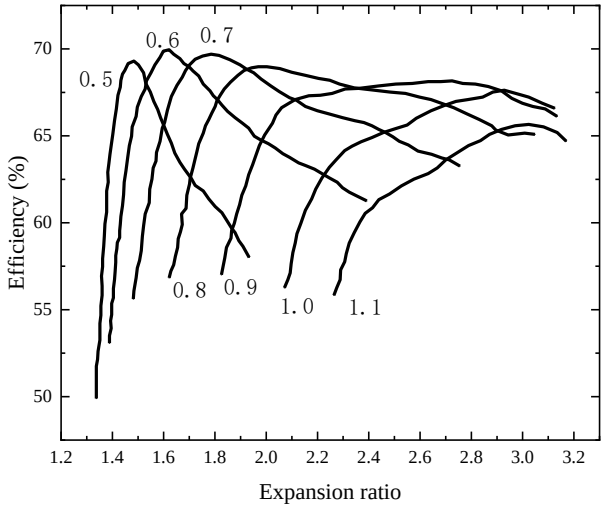

Fig. 6. Performance of turbine.

3.2.4 Sliding bearing

Consumption power of sliding bearing is calculated by Eq (7).

$$P = \frac{2 * \pi * \eta * U^2 * R * L}{c * \sqrt{1 - e^2}} \tag{7}$$

where η is lubricating oil viscosity, U is bearing circumferential velocity, bearing radius R, bearing width L, bearing clearance c and eccentricity ratio e are based on the real geometry.

The governing relation of the shaft dynamic is the energy balance of compressor consumption power, turbine power, load power and sliding bearing consumption power.

$$I\frac{dw}{dt} = W_{\mathrm{t}} - W_c - P + W_e \tag{8}$$

Where W_e can be positive or negative. W_e positive means that high speed permanent motor works, and MGT is in the power consumption state. When W_e is negative, generator works and MGT is in power generation state.

3.2.5 Permanent magnet motor

Permanent magnet motor works as generator and motor, which has the function of starting drive and generation output. Thus, permanent magnet motor operation includes electric operation and power generation operation. When permanent magnet motor operates as a motor, its electric power fluctuates greatly, so it is assumed that the maximum power that the motor output can reach 30kW. It is considered that motor power fluctuates sharply at the critical speed. Therefore, the maximum power of motor is assumed as 15kW. When the permanent magnet motor operates as a generator, its designed power output can reach 40 kW, and the conversion efficiency between mechanical energy and electric power is 0.96, as shown in Eq(9).

$$(W_{\mathrm{t}} - W_{\mathrm{C}} - P) * 0.96 = W_d \tag{9}$$

3.3. Model of self-sustaining state

The power of motor and generator are all zero when the self-sustaining state is achieved, in other words, power of turbine is balanced with the work consumption of compressor and slider bearing, and other work consumption is ignored, as shown in Eq (10).

$$W_{\mathrm{t}} = W_{\mathrm{C}} + P \tag{10}$$

The turbine output power rises with the increase in TIT when the speed remains the same. What's more, the compressor consuming power is not affected by TIT, so provided the TIT is enough high, power from the turbine can always be balanced with the work consumption of compressor and sliding bearing. However, there are restrictions on the MGT. TIT and speed can't exceed the safe value. The designed TIT is 810 ℃ and maximum temperature is 850 ℃.

Based on power performance of MGT, algorithm of self-sustaining state is put forward, as shown in **Fig. 7**. Initial speed is 20,000 rpm, according to characteristics of compressor and turbine. When the relative error between turbine output power and power consumption of compressor and sliding bearing converges to 0.01, it is defined that self-sustaining state is achieved. If self-sustaining state can't be achieved in the 850 ℃, speed is added and then TIT is increased. Self-sustaining state is calculated in this model until speed is at 34,000 rpm.

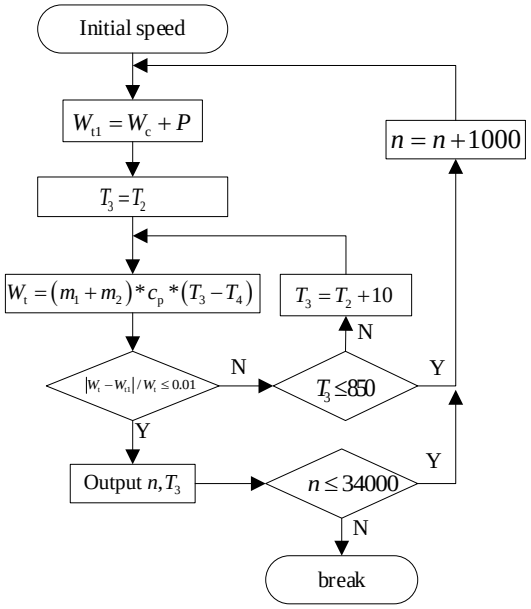

Fig. 7. Model of self-sustaining state.

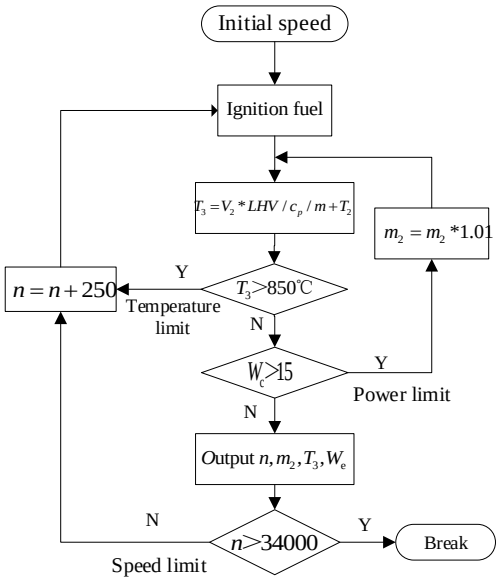

Fig. 8. Model of operation fuel area.

3. 4. Model of operation fuel area

Fuel plays an important role in the MGT start-up process, directly related to the TIT. If the fuel is excessive, the TIT will exceed the temperature of material. On the contrary, when the fuel is too little, the power of motor can not keep the MGT operate normally, or generator power can not meet the need of load. Besides, fuel affects the turbine output power directly. According to the energy conservation, power from turbine and motor needs to meet the demand of work consumption of compressor and sliding bearing, as shown in Eq (11).

$$W_t + W_e = W_c + P \tag{11}$$

Then, the algorithm of operation fuel area is put forward, as shown in **Fig. 8**. Fuel and speed are the independent variable. When the power of motor is over 15 kW, the fuel mass is increased until TIT reaches 850 ℃. If TIT is 850 ℃, then speed is added until speed is 34,000 rpm.

4. Results and discussion

4.1. Numerical analysis of self-sustaining performance

Based on the above model of self-sustaining state, the self-sustaining performance parameters in the temperature 25 ℃ have been calculated. **Fig. 9** and **Fig. 10** give self-sustaining TIT, natural gas and power relation to speed respectively. We can get several conclusions as following.

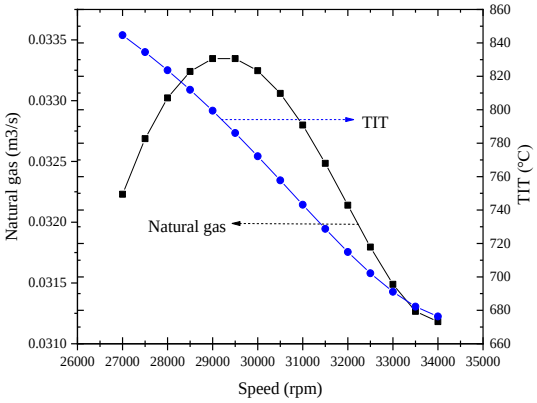

Fig. 9. Self-sustaining TIT and natural gas.

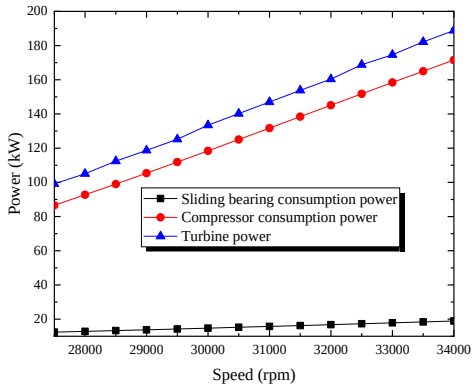

Fig. 10. Self-sustaining power.

There is no more than one self-sustaining state at every speed, as shown in **Fig. 9**. The work consumption of compressor and sliding bearing is constant at one speed when T_1 is unchanged, and the turbine output power is monotonic function of TIT, as shown in Eq (9), so MGT has at most one self-sustaining state at every speed. Furthermore, the first self-sustaining state at the minimum speed of 27,050 rpm means a lot. When the speed is lower, efficiency of compressor is lower, so it cannot reach the self-containing state. On the contrary, the higher speed can have ability to reach the self-containing state easily. However, the self-sustaining TIT decreases when speed increases. There are two reasons. On the one hand, the air mass flow rate increases larger than the natural gas mass rate. On other hand, compressor and turbine efficiency increases when speed increases. However, self-sustaining natural gas increases from

the speed of 27,050 rpm to 29,000 rpm. After the speed of 29,000 rpm, self-sustaining natural gas is decreased. The minimum self-sustaining natural gas happens at the speed of 34,000 rpm because the growth rate of slider bearing power is less than the growth rate of compressor and turbine power.

Fig. 10 shows the power of turbine, compressor and slider bearing relation to rotational speed, which is increased when rotational speed increases. They all increase monotonously with the rotational speed. The consumption power of slider bearing is quadratic function of rotational speed, as shown in Eq (7). Both turbine and compressor consumption power increase larger than slider bearing consumption with the rotational speed. It is obvious that the increase of turbine power is the largest in order to keep MGT self-sustaining with rotational speed.

4.2. Numerical *a*nalysis of operation fuel area during MGT startup

Based on the model of operation fuel area, **Fig. 11** demonstrates turbine power, TIT and natural gas relation to speed respectively at the environment temperature of 25 ℃, whose area is divided into Motor area and Generation area. Motor area means that MGT need to be provided power from motor, whose size is decided by the designed power. Line AF is the boundary of maximum motor power. Generation area means that MGT can offer net power, whose size is mainly determined by the maximum allowable TIT. The boundary CE of motor area and generation area is the self-sustaining line, which is determined by MGT. Boundary BCD represents the restriction of the maximum allowable TIT.

Fig.11 (a) is the turbine power area where MGT keeps safe. The turbine power area is significantly increased after 27,050 rpm, which means that the work capability of turbine is enhanced. Dot line KCE represents the sum consumption power of compressor and sliding bearing. The value in the area ABCEFA minus that in the line KCE equals motor power required to keep MGT operate. The value in the area CDEC minus that in the line CE equals generation power given by load.

Fig. 11 (b) shows TIT allowable operation area. The tendency of motor area in Fig. 11 (b) is different from that in Fig.11 (a). It is obvious that TIT area narrows with rotational speed in the motor aera, because compressor consumption power is increased,

but the maximum motor power is constant. In other words, the effect of motor on MGT is gradually diminished and lastly replaced by generator, which is agreement with the fact.

Fig. 11 (c) represents natural gas operation area, whose tendency is similar that in Fig. 11 (a). natural gas area is not only related with maximum allowable TIT and motor power, but also related with LHV. High LHV lead to small fuel operation area. Therefore, the analysis of operation area is more significant if MGT uses different fuels.

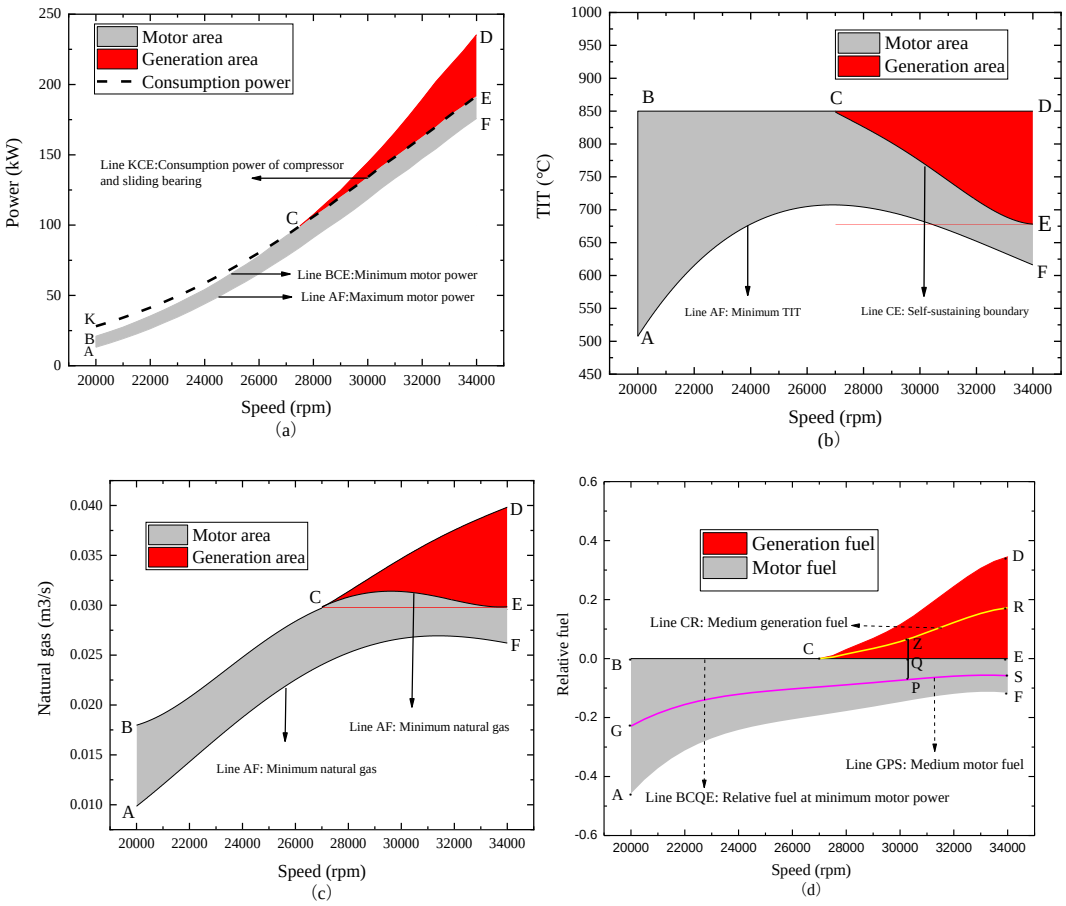

Fig. 11. Self-sustaining operation area during the start-up.

4.3. Determination of SSP in the MGT start-up process

Self-sustaining state can be reached at the rated speed or non-rated speed. Operation fuel area is different in the two self-sustaining speed mode. It is convenient to take maximum fuel flow rate in the motor state as relative adjustment of fuel benchmark. **Fig. 11 (d)** shows relative operation fuel in the start-up process. Relative adjustment of fuel benchmark is defined as Rf. If Rf is positive, MGT is in the generation state. On

the contrary, when Rf is negative, MGT is in the motor state. Point D is the design point. Line GPS is the median line of the motor fuel operation area, which is between the maximum value and the minimum value of the motor fuel. Similarly, line CR is the median line of the power generation fuel operation area, which is between the maximum value and the minimum value of the generation fuel. Generation area is same big as the motor area at the speed of 30,250 rpm, where point P and Z are median value of motor area and generation area respectively. Point Q is the sustaining state at 30,250 rpm. When speed is over 30,250 rpm, generation area is bigger than motor area. On the contrary, if speed is less than 30,250 rpm, motor area is bigger.

No matter what kind of self-sustaining speed mode is chosen, point D is the target in **Fig. 11 (d)**. Point G, R and S are the midpoint of line AB, DE and EF. The greater the relative adjustment of fuel, the higher the safety of the operation of MGT. Then, based on the principle of maximum fuel regulation margin, typical way G-P-Q-Z-R-D and G-P-S-E-D are compared. Fuel regulation margin is in way P-Q-R rises with the speed increasing. However, fuel regulation margin of way P-S decreases when the speed increases. The maximum fuel regulation margin in way P-Q-R is three times larger than that in way P-S. As a result, way G-P-Q-Z-R-D is determined and the SSP is selected at the speed of 30,250 rpm.

4.4. Self-sustaining performance verification

Self-sustaining experiment is made at different speed in the environment temperature 26 ℃. Self-sustaining state is defined to be reached when both the power of motor and generator are below 0.3 kW. The comparison of experimental and theoretical calculation is shown in **Fig. 12**. Self-sustaining state is reached at the speed of 28,000 rpm, 29,000 rpm, 30,000 rpm, 31,000 rpm, 32,000 rpm, 33,000 rpm, 34,000 rpm. Compared with theoretical results, the relative difference of TIT is within 2.4%, as shown in **Fig. 12(a)**. The maximum absolute difference happens at the speed of 34,000 rpm, arriving at 16℃ and the relative error is just 2.35%. However, design temperature is 810 ℃, and the maximum temperature is 850 ℃, so the reasonable difference of temperature can reach 35 ℃, which means the theoretical calculation is reasonable.

What's more, **Fig. 12(b)** shows that the relative difference of natural gas mass is within 4% and the maximum relative error is 3.41% at the speed of 28,000 rpm, which is also acceptable.

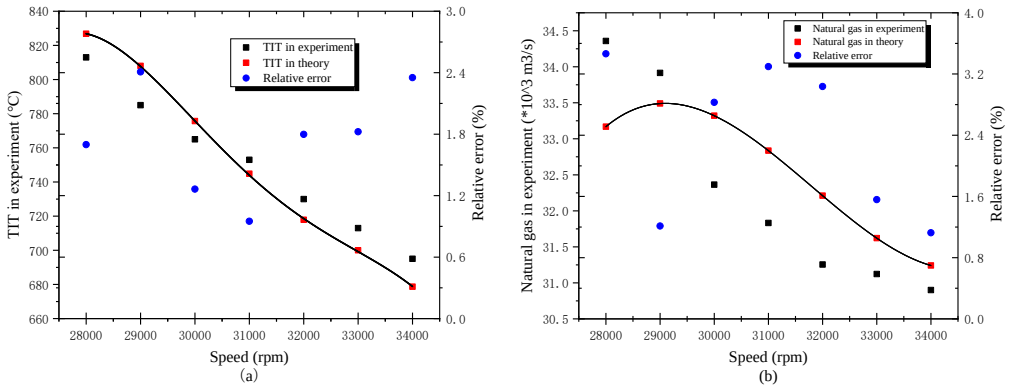

Fig. 12. The comparison of experiment and theoretical calculation.

Self-sustaining experiment is not only made in the same temperature, but also in the different temperature. Due to the fact that environment temperature is natural, then self-sustaining state has been respectively got in the temperature 22 ℃, 24 ℃, 26 ℃ and 32 ℃ at the speed of 31,000 rpm. The comparison of experimental data and theoretical results are shown in **Table 2**. The maximum relative error of TIT happens at 24 ℃, which is 1.23%, where the maximum relative error of natural gas is 3.12%. Above all, the relative difference of TIT is within 2% and that of natural gas mass is within 4%, which is also acceptable. So, algorithm of self-sustaining state is effective in different temperature.

Table 2.
Experimental data and theoretical results in different environment temperature.

T_1/ ℃	TIT experiment /℃	TIT theory/℃	Relative error/%	V_2 experiment/ $\times 10^3$ m^3/s	V_2 theory/ $\times 10^3$ m^3/s	Relative error/%
22	730.1	735.3	0.73	31.85	32.6	2.35
24	732.3	741.1	1.23	31.78	32.77	3.12
26	753.2	745.8	-0.96	32.05	32.88	2.58
32	770.5	751.1	-1.17	33.92	33.42	-1.48

4.5. Startup experiment from speed 0 to speed 29000

The experiments of self-sustaining state and maximum generation are made at the speed of 29,000 rpm in the temperature 30 ℃. **Fig. 13** shows the complete process of

electric power from static state to the maximum generation state. It is clear that when the permanent magnet motor works as a motor, its power fluctuates greatly, which is consistent with hypothesis. The rotational speed increases in steps. Ignition happens at the rotational speed of 6000 rpm. The TIT changes huge, but the motor power has little decrease. This is because the work capability of turbine is weak when the rotational speed is low. After 6000 rpm, the motor is increasing step by step. It is obvious that the abrupt change happens at the time of 610s. This change is between the rotational speed of 12,000 rpm to 16,000 rpm. The motor power even exceeds over 15kW. This results from that the critical rotational speed is between the rotational speed of 12,000 rpm to 16,000 rpm, which must be crossed quickly, or equipment is damaged. After the rotational speed of 20,000 rpm, the motor power is stable around the 10 kW. The motor power is decreased step by step when the rotational speed is at 29,000 rpm until MGT enters the generation state. MGT promotes generation power from 0 kW to 5 kW.

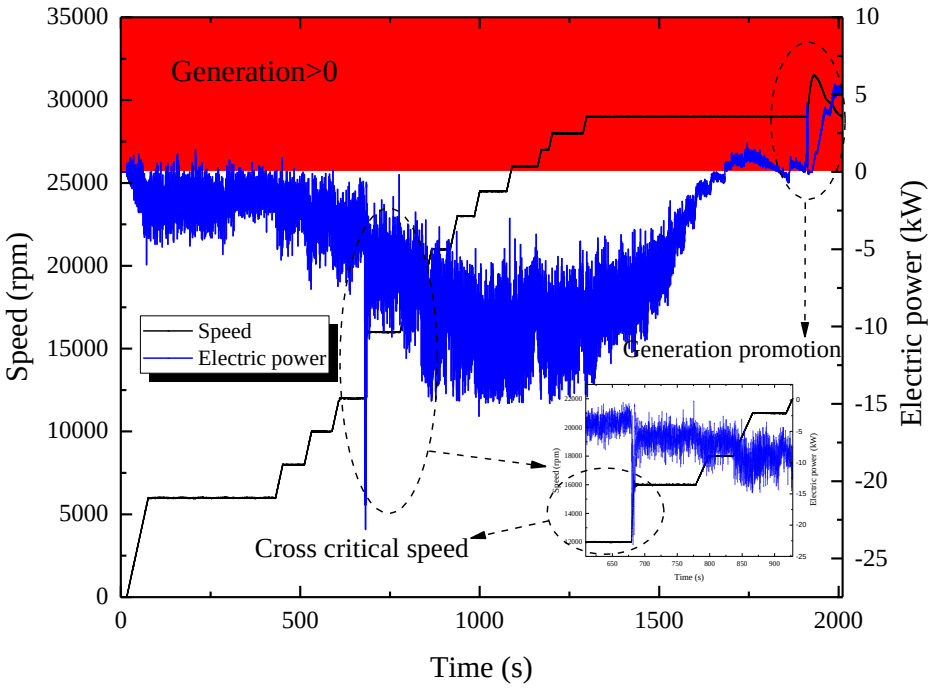

Fig. 13. The complete process of electric power.

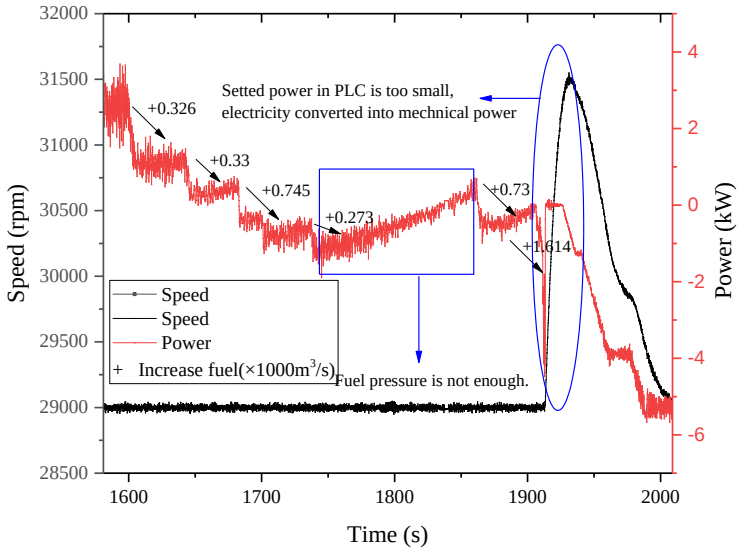

Fig. 14. The power promotion at the speed of 29,000 rpm.

Fig. 14 shows the power promotion at the set speed of 29,000 rpm from motor state to maximum generation state. In this process, fuel is particularly important. By increasing the fuel, the power of the motor is reduced. It is obvious that the fuel is not proportional to power. MGT goes into the state of generating electricity by adding fuel three times. However, due to rapid consumption of fuel, the pressure of gas tank can not maintain the power. As a result, the state is from generation state switched to motor state from the time 1748s to the time 1850s. Then, the valve opens wider to supply enough fuel to the combustor. MGT arrives the generation state again. After MGT has the ability to generate electricity, load must match with the amount of fuel, or the speed will change with the amount of fuel. The motor power can reach 0.3 kW at the time1860 s. when the time is at 1910 s, power is sharply decreased because the MGT can make generation, but the load is not set. The power is converted to mechanical power and then the speed is increased to 31,500 rpm. After the load power of 5 kW is set up, the generation power is up to 5.24 kW and the TIT is 849.5 ℃.

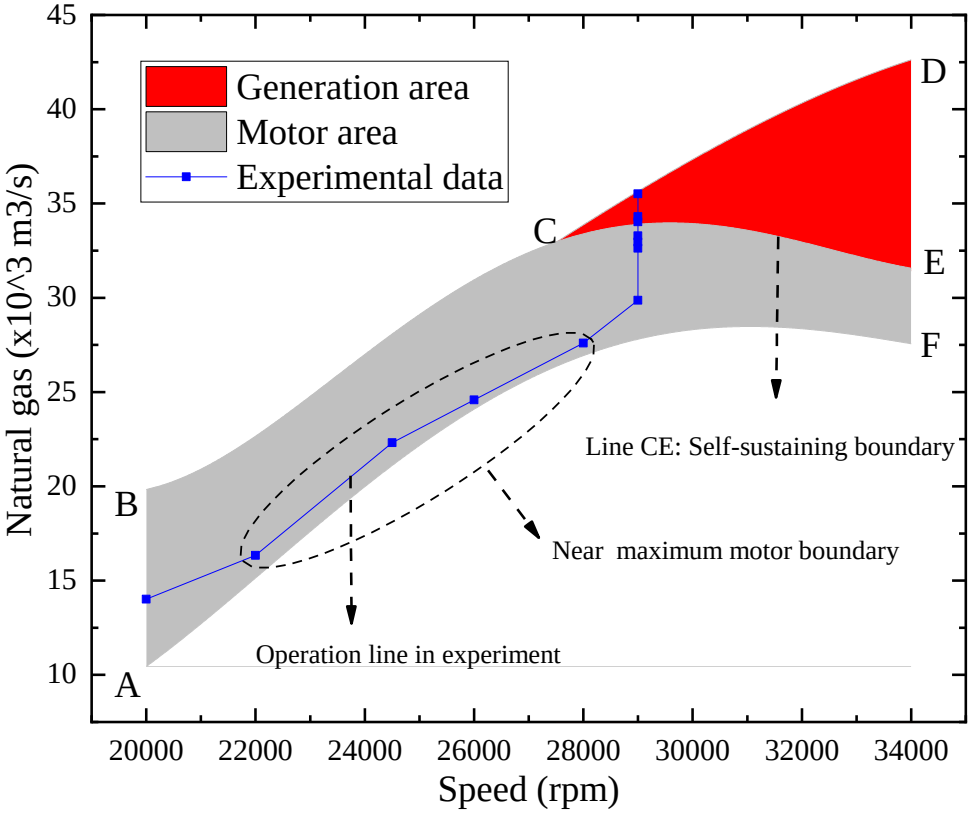

Fig. 15. Natural gas in the temperature 30 ℃.

Fig. 15 shows that natural gas mass from speed of 20,000 rpm at every speed is in the operation fuel area. From the **Fig. 13**, the motor power fluctuates around 10 kW from the rotational speed 22,000 rpm to 28,000 rpm. Accordingly, the fuel is close to the fuel operation boundary, as shown in **Fig. 15.** Fuel is gradually increased at the rotational speed of 29,000 rpm. as a result, the motor decreased significantly until it drops to 0. When the natural gas flow is maximum, the electric is also maximum.

Fig. 16 and **Fig. 17** shows comparison of TIT and power of motor or generator based on the experimental and theoretical results. The parameters are so much that a relative benchmark must be established before comparisons can be made. There, the principle is that keep the TIT and speed of experimental and theoretical results close and compare the power of motor or generator. **Fig. 16(a)** is the TIT from the rotational speed 20,000 rpm to the first step at 29,000 rpm. **Fig. 16(b)** is the process promoting TIT at 29,000 rpm. The tendency of TIT almost keeps increasing, especially in **Fig. 16(b),** which means that generation must have enough TIT. The relative difference of

TIT is within 0.5%. So, the TIT of experimental and theoretical results can be regarded as the same. **Fig. 17(a)** is the electric power from the rotational speed 20,000 rpm to the first step at 29,000 rpm. **Fig. 17(b)** are the electric power process from motor power switching to generation. The motor power is decreased sharply at the 29,000 rpm. The relative error of motor power is within 5% in **Fig. 17(a)**. However, the maximum relative difference of power of electric power is about 30%. The reason is that the absolute power is just 0.67 kW and the fluctuation is within 0.2 kW, which is acceptable.

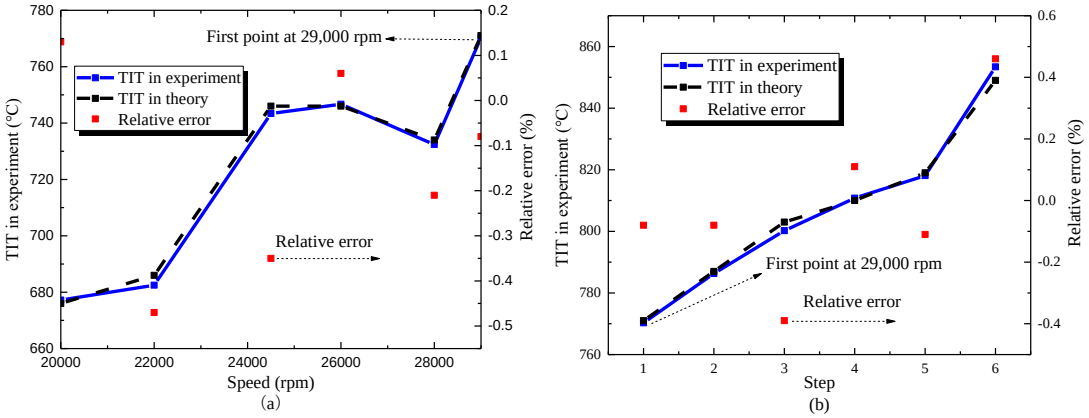

Fig. 16. The comparison of TIT in experiment and theory.

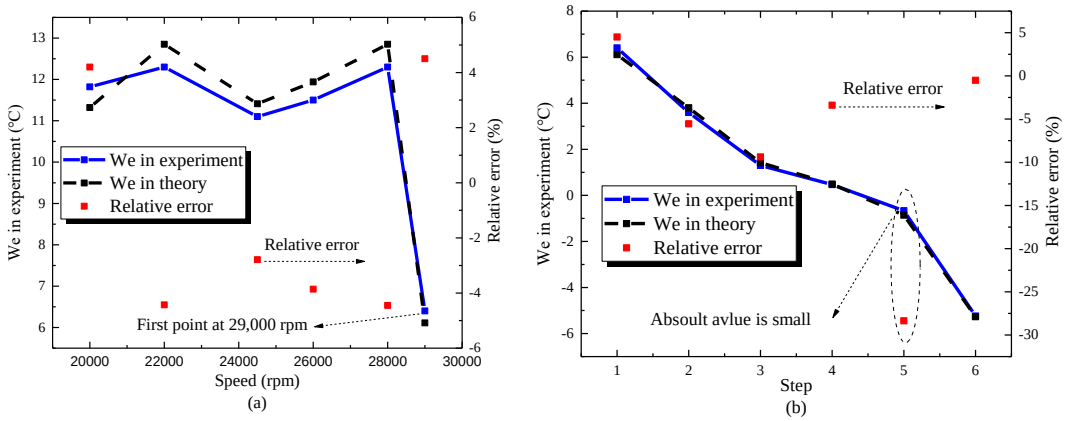

Fig. 17. The comparison of electric power in experiment and theory.

5. Conclusion

This work is based on the self-designed 40 kW MGT generation system. According to the characteristic of MGT, startup schedule is analyzed. Self-sustaining performance is calculated based on the performance maps of components. Furthermore, SSP is

determined based on the principle of maximum adjustable operation margin. Lastly, the complete experiment of MGT is used to testify the accuracy of algorithm of self-sustaining state and operation fuel area. Through investigations, some meaningful results are obtained.

(1) The whole start-up process contains motor startup, ignition, speed acceleration, motor switching to generator and power acceleration. Self-sustaining state is one of the most important state during the startup, when motor switching to generator happens. Self-sustaining state at the continuous speed forms the self-sustaining boundary.

(2) Only if speed arrives at special speed, self-sustaining state can be reached. Self-sustaining state is reached at the speed of 27,050 rpm in the self-designed MGT, and above the 27,050 rpm, self-sustaining state all can be reached. However, no matter how to adjust the fuel quantity, it can't reach self-sustaining state when speed is less than 27,050 rpm. What's more, minimum self-sustaining speed is decreased with T_1 decreasing.

(3) Generation area is enlarged when speed increases. On the contrary, fuel area in motor is reduced. Compared with operation fuel area at rated speed, operation area at unrated speed is larger. According to maximum adjustable fuel principle, operation way G-P-R-D1 is determined and the self-sustaining speed is 30,250 rpm.

(4) The maximum relative error between the theoretical calculation of turbine inlet temperature and the experimental temperature is 2.4%, and the maximum relative error of fuel is 3.41% in environmental temperature of 26 ℃. The maximum power generation calculated theoretically is 5.27 kW at 29,000 rpm, where the actual power generation reaches 5.24 kw, and the relative error is only 0.57%. What's more, the relative error of TIT and fuel quantity is within 4%, which can be used as reference value in practical operation.

Acknowledgements

The research is supported by National Natural Science Foundation of China under Grant No. 51806137, and Shanghai Rising- Star Program under Grant No. 20QA1404700.

References

[1] J. Chen, C. Zhou, S. Wang, S. Li, Impacts of energy consumption structure, energy intensity, economic growth, urbanization on PM2.5 concentrations in countries globally, Applied Energy, 230 (2018) 94-105.

[2] Z. Cheng, L. Luo, S. Wang, Y. Wang, S. Sharma, H. Shimadera, X. Wang, M. Bressi, R.M. de Miranda, J. Jiang, W. Zhou, O. Fajardo, N. Yan, J. Hao, Status and characteristics of ambient PM2.5 pollution in global megacities, Environ Int, 89-90 (2016) 212-221.

[3] World Energy Council, Global Energy Comparison Review, World Energy Insights Brief 2019, London, 2019. April 2019..

[4] World Energy Council, World Energy Scenarios 2019 – Exploring Innovation Pathways to 2040, in Collaboration with Accenture Strategy and, Paul Scherrer Institute, London, 2019. September 2019..

[5] T. Kober, H.W. Schiffer, M. Densing, E. Panos, Global energy perspectives to 2060 – WEC's World Energy Scenarios 2019, Energy Strategy Reviews, 31 (2020).

[6] K.A. Al-attab, Z.A. Zainal, Performance of a biomass fueled two-stage micro gas turbine (MGT) system with hot air production heat recovery unit, Applied Thermal Engineering, 70 (2014) 61-70.

[7] K.A. Al-attab, Z.A. Zainal, Micro gas turbine running on naturally aspirated syngas: An experimental investigation, Renewable Energy, 119 (2018) 210-216.

[8] A. Cavarzere, M. Morini, M. Pinelli, P.R. Spina, A. Vaccari, M. Venturini, Experimental Analysis of a Micro Gas Turbine Fuelled with Vegetable Oils from Energy Crops, Energy Procedia, 45 (2014) 91-100.

[9] S. Giorgetti, A. Parente, L. Bricteux, F. Contino, W. De Paepe, Optimal design and operating strategy of a carbon-clean micro gas turbine for combined heat and power applications, International Journal of Greenhouse Gas Control, 88 (2019) 469-481.

[10] A. Liu, Y. Yang, L. Chen, W. Zeng, C. Wang, Experimental study of biogas combustion and emissions for a micro gas turbine, Fuel, 267 (2020).

[11] X. Lv, X. Ding, Y. Weng, Effect of fuel composition fluctuation on the safety performance of an IT-SOFC/GT hybrid system, Energy, 174 (2019) 45-53.

[12] X. Wang, X. Lv, Y. Weng, Performance analysis of a biogas-fueled SOFC/GT hybrid system integrated with anode-combustor exhaust gas recirculation loops, Energy, 197 (2020).

[13] L. Aichmayer, J. Garrido, B. Laumert, Thermo-mechanical solar receiver design and validation for a micro gas-turbine based solar dish system, Energy, 196 (2020).

[14] G.B. de Campos, C. Bringhenti, A. Traverso, J.T. Tomita, Thermoeconomic optimization of organic Rankine bottoming cycles for micro gas turbines, Applied Thermal Engineering, 164 (2020).

[15] M.J. Kim, T.S. Kim, Integration of compressed air energy storage and gas turbine to improve the ramp rate, Applied Energy, 247 (2019) 363-373.

[16] A. Karvountzis-Kontakiotis, A.M. Andwari, A. Pesyridis, S. Russo, R. Tuccillo, V. Esfahanian, Application of Micro Gas Turbine in Range-Extended Electric Vehicles, Energy, 147 (2018) 351-361.

[17] P. Jansohn, Overview of gas turbine types and applications, Modern Gas Turbine Systems2013, pp. 21-43.

[18] J. Yuan, C. Cui, Z. Xiao, C. Zhang, W. Gang, Performance analysis of thermal energy storage in distributed energy system under different load profiles, Energy Conversion and Management, 208 (2020).

[19] A. di Gaeta, F. Reale, F. Chiariello, P. Massoli, A dynamic model of a 100 kW micro gas turbine fuelled with natural gas and hydrogen blends and its application in a hybrid energy grid, Energy, 129 (2017) 299-320.

[20] M.J. Kim, J.H. Kim, T.S. Kim, Program development and simulation of dynamic operation of micro gas turbines, Applied Thermal Engineering, 108 (2016) 122-130.

[21] E. Tsoutsanis, N. Meskin, Dynamic performance simulation and control of gas turbines used for hybrid gas/wind energy applications, Applied Thermal Engineering, 147 (2019) 122-142.

[22] President W E B F . Gas turbine control and protection[J]. Forsthoffer's Rotating Equipment Handbooks, 2005, 1(4225):439-454.

[23] David Pritchard, Biomass fuelled indirect fired micro turbine, B/Tl/00790/00/00/REP, DTI/Pub URN. 05/698, Talbott's Heating Ltd, First Published 2005.

[24] K.A. Al-attab, Z.A. Zainal, Turbine startup methods for externally fired micro gas turbine (EFMGT) system using biomass fuels, Applied Energy, 87 (2010) 1336-1341.

[25] H. Asgari, X. Chen, M. Morini, M. Pinelli, R. Sainudiin, P.R. Spina, M. Venturini, NARX models for simulation of the start-up operation of a single-shaft gas turbine, Applied Thermal Engineering, 93 (2016) 368-376.

[26] Kim J H , Song T W , Kim T S , et al. Dynamic Simulation of Full Startup Procedure of Heavy-Duty Gas Turbines[J]. Journal of Engineering for Gas Turbines & Power, 2002, 124(3):510-516.

[27] P.K. Mohammadian, M.H. Saidi, Simulation of startup operation of an industrial twin-shaft gas turbine based on geometry and control logic, Energy, 183 (2019) 1295-1313.

[28] P. Lin, X. Du, Y. Shi, X.M. Sun, Modeling and controller design of a micro gas turbine for power generation, ISA Trans, (2020).

[29] A. Mehrpanahi, A. Hamidavi, A. Ghorbanifar, A novel dynamic modeling of an industrial gas turbine using condition monitoring data, Applied Thermal Engineering, 143 (2018) 507-520.

[30] Pritchard D. Biomass combustion gas turbine CHP[J]. Staffordshire, UK, 2002.

[31] J. Seo, H.-S. Lim, J. Park, M.R. Park, B.S. Choi, Development and experimental investigation of a 500-W class ultra-micro gas turbine power generator, Energy, 124 (2017) 9-18.

[32] N. Badshah, K.A. Al-attab, Z.A. Zainal, Design optimization and experimental analysis of externally fired gas turbine system fuelled by biomass, Energy, 198 (2020).